

OPF-HGNN: Generalizable Heterogeneous Graph Neural Networks for AC Optimal Power Flow

Salah GHAMIZI
LIST, Member, IEEE

Esch-Belval, Luxembourg

<https://orcid.org/0000-0002-0738-8250>

Aoxiang MA
LIST

Esch-Belval, Luxembourg

<https://orcid.org/0009-0005-9553-5650>

Jun CAO
LIST, Member, IEEE

Esch-Belval, Luxembourg

<https://orcid.org/0000-0001-5099-9914>

Pedro RODRIGUEZ CORTES
LIST, University of Luxembourg, Fellow, IEEE

Esch-Belval, Luxembourg

<https://orcid.org/0000-0002-1865-0461>

Abstract—The precise solution of the Alternating Current Optimal Power Flow (AC-OPF) problem is a pivotal challenge in the domain of real-time electricity grid operations. This problem is notorious for its significant computational complexity, primarily attributable to its inherently nonlinear and nonconvex nature. Recently, there has been a growing interest in harnessing Graph Neural Networks (GNN) as a means to tackle this optimization task, leveraging the incorporation of grid topology within neural network models. Nonetheless, existing techniques fall short in accommodating the diverse array of components found in contemporary grid networks and restrict their scope to homogeneous graphs. Furthermore, the constraints imposed by the grid networks are often overlooked, resulting in suboptimal or even infeasible solutions. To address the generalization and effectiveness of existing end-to-end OPF learning solutions, we propose OPF-HGNN, a new graph neural network (GNN) architecture and training framework that leverages heterogeneous graph neural networks and incorporates the grid constraints in the node loss function using differentiable penalty regularization. We demonstrate that OPF-HGNN is robust and outperforms traditional GNN learning by two orders of magnitude traditional GNN learning across a large variety of real-world grid topologies and generalization settings.

Index Terms—OPF, Graph Neural Network, Heterogeneous GNN, Robustness, Physics-Informed.

I. INTRODUCTION

Solving Optimal Power Flow (OPF) problems is a routine task in power systems (PS) operational planning. However, accurately solving these problems, considering the growing variability, constraints, and uncertainties in modern power systems, also represents a serious challenge for power system engineers. OPF is basically an optimization problem aimed at identifying the optimal voltage set-points at system buses and the power output of generators to meet load demands, while complying with the technical and operational constraints of PS and maximizing efficiency in power transmission, thereby minimizing losses and costs. Many contemporary approaches to tackling the AC OPF problem leverage machine learning (ML) components to balance the computational complexity inherent in traditional optimization-based OPF methods.

Although most ML techniques use fully connected neural networks (FCNN) [3], a growing literature has tackled the

applications of Graph Neural Networks (GNN) to account for the topology and reduce the size of the model [1], [8], [10].

GNN has recently demonstrated solid performance for various tasks in the power system, including fault detection and isolation [6], prediction of power outages [5], and optimal power flow [10]. They are trained with network states as input to approximate optimal solutions power and voltage. The seminal work of Owerko et al. [10] on OPF demonstrated their effectiveness in using latent grid structures and outperforming traditional methods.

GNN for OPF still faces two main challenges, namely system constraint satisfaction (e.g., voltage limits) and topology generalization. The former is heavily investigated through the lens of physics-informed neural networks [4], where the constrained domain is injected into the ML model, either through regularization, custom loss function, or dedicated architectures. The second challenge has been scarcely explored and was recently initiated by Liu et al. [9]. In their work, they unveiled a new topology-informed GNN approach by integrating grid topology and physical constraints.

However, these GNN approaches for OPF lean on the homogeneous neural network paradigm, where the nodes of the graph are the buses and the edges of the graph are the lines and substations. We argue that such representation oversimplifies the power system. Such a representation squanders a significant amount of data pertaining to the nodes and fails to accommodate the diverse range of components within a modern grid. Indeed, the static and dynamic properties of loads, lines, external grids, generators, etc. are all merged in the bus node's representation in the traditional homogeneous GNNs. This simplification also hinders the GNN from taking into account the individual constraints components. Donon et al. [1] proposed a neural solver that relies on heterogeneous graphs to minimize the violation of Kirchhoff's laws and not the error to the optimal AC flow solutions of the solvers.

Our work ¹, to the best of our knowledge, is the first

¹This work was supported by FNR CORE project LEAP (17042283), and the implementation code is available at <https://github.com/yamizi/OPF-HGNN>

to suggest a novel heterogeneous graph representation of the power grid for AC-OPF and proposes a representation where all components and their specific features and domain constraints are supported. We present in Figure 1 how a 9-bus power grid can be simplified as a homogeneous graph and how our approach extends it to a heterogeneous graph. The contributions of our work are threefold, as summarized here.

- We propose a heterogeneous GNN-based topology generalizable framework for OPF learning. We demonstrate that our approach, OPF-HGNN, can embed a wider set of heterogeneous components in power systems.
- We hypothesize that OPF-HGNN supports ac feasibility and network constraint satisfaction with a novel constraint satisfaction regularization mechanism embedded in the representation of the node.
- We demonstrate through a representative empirical study that OPF-HGNN outperforms homogeneous graph representation, is robust to power grid mutations, and can generalize to load and cost variations across multiple real-world topologies.

II. OUR APPROACH

A. Problem Formulation

The AC-OPF problem is formulated as follows:

$$\min_{p,q,v} \sum_{i=1}^N c_i(p_i) \quad (1)$$

$$\text{s.t. } p + jq = \text{diag}(v)(Xv)^*, \quad (2)$$

$$V_{\min} \leq |v| \leq V_{\max}, \quad (3)$$

$$p_{\min} \leq p \leq p_{\max}, \quad q_{\min} \leq q \leq q_{\max}, \quad (4)$$

$$s_{ij}(v) \leq \bar{s}_{ij}, \quad \forall (i, j) \in \mathcal{E}. \quad (5)$$

where:

- p and q are the vectors of active and reactive power injections at each node, respectively.
- $c_i(p_i)$ represents a cost curve that is monotonically increasing and convex.
- X is the given network admittance matrix (X -bus).
- v is the vector of complex nodal voltages.
- V_{\min} and V_{\max} are the specified lower and upper voltage magnitude limits, respectively.
- p_{\min} , p_{\max} , q_{\min} , and q_{\max} are the lower and upper bounds for active and reactive power injections.
- $s_{ij}(v)$ denotes the apparent power flow on line (i, j) , and \bar{s}_{ij} is the corresponding limit.
- (\mathcal{E}) denotes the set of power lines in the network.

Our approach aims to predict with a graph neural network the pairs p, q for each generator that minimizes the objective function and enforces the domain constraints.

B. Heterogenous Graph Neural Networks

Traditional message passing GNN [2], [7] cannot trivially deal with heterogeneous graph data. This is because the inherent differences in feature across nodes and edges make it non-straightforward to apply the same processing functions.

Constraints formulae	Penalty function
$\omega_1 \wedge \omega_2$	$\omega_1 + \omega_2$
$\omega_1 \vee \omega_2$	$\min(\omega_1, \omega_2)$
$\psi_1 \leq \psi_2$	$\max(0, \psi_1 - \psi_2)$
$\psi_1 < \psi_2$	$\max(0, \psi_1 - \psi_2 + \epsilon)$

TABLE I: The grammar used to convert constraint formulae to penalty functions where ϵ is an infinitesimal value.

We extend it to support multiple type nodes by interleaving the message functions on each edge type individually. We present in figure 2 the extension of a standard single node type architecture to two node types (bus and load). Our OPF-HGNN supports 11 types of nodes, each with a specific set of features to describe the component and its boundaries.

Let \mathcal{N} be the set of nodes of our power grid, and \mathcal{E} be the edge dictionary. The set of node features denoted as $\mathcal{X} = \{x_v, \forall v \in \mathcal{N}\}$ encompasses the attributes of each node, the type of attribute depends on the type of node (bus, line, load, etc.). In addition to the node features, the subset of generator nodes, denoted \mathcal{G} , is also defined by a set of boundary constraints $\{\Omega_g, \forall g \in \mathcal{G}\}$ and its true active and reactive powers at OPF $\hat{y} = \{\hat{y}_g, \forall g \in \mathcal{G}\}$. The GNN's layers are GraphSage [2] convolutional layers. The output of our GNN is a 2-output linear regression layer for each generator node $y = \{y_g, \forall g \in \mathcal{G}\}$. The output of every generator node predicts the optimal active and reactive power injections that each generator should have at OPF. The first objective of training the GNN is then to minimize the error between these predicted values y and their ground truths \hat{y} .

C. Constraint Regularization

The second objective of the learning is to account for the boundary constraints of the OPF problem. We incorporate these constraints in the loss of our GNN as regularization terms. We transform each of the constraints in Equation (4) into a penalty function following the grammar in Table I [11], [12]. Given a training graph features \mathcal{X} , its associated ground truth prediction \hat{y} and its predicted output y , the training loss function of our GNN (parametrized by Θ) becomes:

$$\mathcal{L}(\Theta) := \sum_{g \in \mathcal{G}} \left[\|y_g - \hat{y}_g\|_2^2 + \lambda \sum_{\omega_i \in \Omega_g} \text{penalty}(x_g, \omega_i) \right] \quad (6)$$

where the second term captures the weighted constraints violations of the power grid given the set of constraints Ω_g .

D. Graph Mutation

Our goal is to achieve a generalizable GNN, hence we design two data augmentation mechanisms based on feasible graph mutations. Starting from a feasible graph where the OPF can converge with a simulation toolkit, we randomly mutate the loads and generators with a mutation rate τ :

Cost mutation: For each of the generators, we mutate the cost coefficients c_i with a random number between the minimum and maximum cost boundaries $c_{i,\min}$ and $c_{i,\max}$ for all existing generators. This mutation reflects scenarios

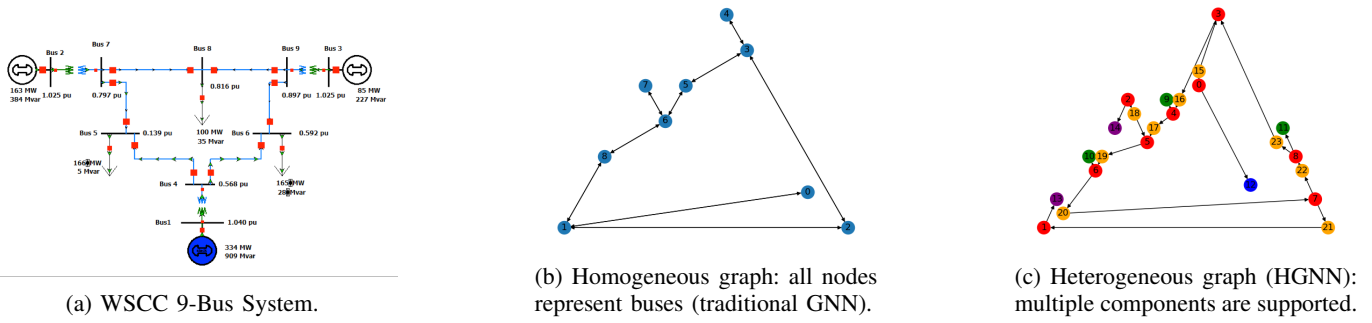


Fig. 1: Illustrative comparison of network representation for the same power grid WSCC 9-Bus: (a) WSCC 9-Bus System; (b) Homogeneous graph where all nodes represent buses and the edges are the lines; (c) Heterogeneous graph where node colors correspond to different network components: Red for Buses, Green for Loads, Blue for External Grid, Purple for Generators, and Orange for Lines. Our OPF-HGNN approach emphasizes the diversity of components of modern power systems.

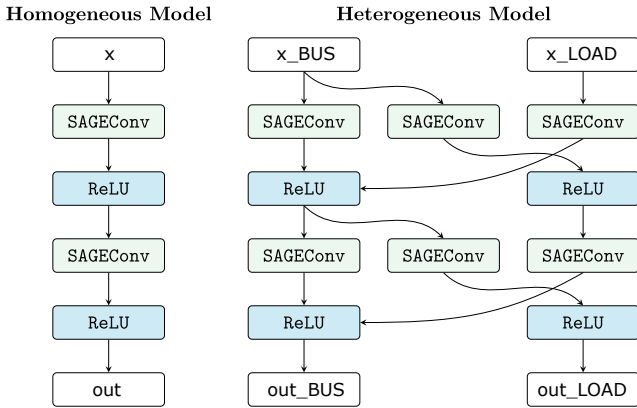


Fig. 2: Transforming a homogeneous GNN to a heterogeneous GNN by combining message passing across multiple types. In this example with two node types **bus** and **load**.

where some generator types (e.g., gas) become expensive and require new routing scenarios.

Load mutation: For each load L_i , we mutate its active power P_{L_i} and reactive power Q_{L_i} with a multiplicative coefficient drawn from a uniform distribution. This mutation reflects scenarios with unexpected peaks or drops of consumption.

Following the node mutation, we rebuild our network and optimize the OPF using a simulation toolkit. If the simulation fails or the OPF does not converge, we discard this mutant and generate a new one. We also discard a graph from the validation set if its signature matches the signature of a graph from the training set to avoid training validation leakage.

Following our mutation operators, we generate the ground truth of the OPF for each graph using the simulation tool.

E. OPF-HGNN Algorithm

The proposed OPF-HGNN framework is summarized in the Algorithm 1. Lines 4-6 are for the mutation and simulation of our topologies, lines 7-14 are for the embedding generation, and lines 15-18 are for the loss computation used in backpropagation to update the weights of the model.

Algorithm 1 OPF-HGNN training of power grid $(\mathcal{N}, \mathcal{E})$

Require: training graph $\mathbb{G}_t(\mathcal{N}, \mathcal{E})$;
Require: depth K ; weight matrices $W^k, \forall k \in \{1, \dots, K\}$;
Require: aggregators $\text{AGGREGATE}_k, \forall k \in \{1, \dots, K\}$;
Require: set of validation graphs $\mathcal{V} = \{\mathbb{G}_v(\mathcal{N}, \mathcal{E})\}$;
Require: neighborhood function $\mathcal{N} : v \rightarrow 2^{\mathcal{N}}$;

- 1: $l \leftarrow 0$ ▷ Initialize the epoch loss
- 2: **for** $m = 1$ **to** M : **do**
- 3: **do**
- 4: $\mathbb{G}_v \leftarrow \text{MUTATE}(\mathbb{G}_t, \mu)$
- 5: valid, $\{x_{m,v}\}, \{\hat{y}_{m,g}\}, \{\Omega_g\} \leftarrow \text{SIMULATE}(\mathbb{G}_v)$
- 6: **while** $\mathbb{G}_v \in \mathcal{V}$ or \neg valid
- 7: $h_v^0 \leftarrow x_{m,v}, \forall v \in \mathcal{N}$
- 8: **for** $k = 1 \dots K$: **do**
- 9: **for** $v \in \mathcal{N}$: **do**
- 10: $h_{\mathcal{N}(v)}^k \leftarrow \text{AGGREGATE}_k(\{h_u^{k-1}, \forall u \in \mathcal{N}(v)\})$
- 11: $h_v^k \leftarrow \text{RELU}(W^k \cdot \text{CONCAT}(h_v^{k-1}, h_{\mathcal{N}(v)}^k))$
- 12: **end for**
- 13: $h_v^k \leftarrow h_v^k / \|h_v^k\|_2, \forall v \in \mathcal{N}$
- 14: **end for**
- 15: $\{y_{m,g}\} \leftarrow \text{LINEAR}(\{h_v^K, \forall v \in \mathcal{N}\})$ ▷ Regression
- 16: $l_{mse} \leftarrow \text{MSE}(\{y_{m,g}\}, \{\hat{y}_{m,g}\})$
- 17: $l_{penalty} \leftarrow \text{PENALTY}(\{y_{m,g}\}, \{\Omega_g\})$
- 18: $l \leftarrow l + (l_{mse} + \lambda \cdot l_{penalty})$ ▷ Weighted penalty
- 19: **end for**
- 20: ▷ Update weight matrices W^k by backpropagation of l

III. EMPIRICAL STUDY

A. Experimental Protocol

a) *Use case:* We evaluate three commonly used topologies: WSCC 9-Bus system, IEEE 14-Bus system, and IEEE 30-Bus system. The first case represents a simple system with 9 buses, 3 generators, and 3 loads.

The IEEE test cases represent an approximation of the American Electric Power system. The IEEE 14-bus system has 14 buses, 5 generators, and 11 loads, and the IEEE 30-Bus system has 15 buses, 5 generators, and 24 loads.

b) *Simulation tool:* We use PandaPower [13] for topology validation, power flow simulation, and OPF ground truth generation. We integrate this tool into the data augmentation pipeline through its Python API. For each use case, we mutate the network and simulate the mutants to generate the training and validation set. The performance study uses 8.000 training mutants and 2.000 validation mutants.

c) *Neural Network architecture*: We evaluate three ML models for OPF learning. The first baseline is a fully connected neural network (FCNN) where the features of all the nodes of the graphs are concatenated into one input. In the WSCC 9-Bus case, for example, this model is trained on 360 features. The FCNN has two fully connected layers with relu activations after each and one output layer with two regression outputs per generator (i.e. in the WSCC 9-Bus case 6 outputs).

The second baseline is the homogeneous graph neural network (GNN), the common approach to implement power systems in graph neural networks. The model is made of two SageGraph convolution layers followed by relu activations and one final layer with two outputs per bus node (i.e., in the WSCC 9-Bus case, 18 outputs). The training loss computation takes into account the features of all the nodes (9 nodes x 40 features), but only the output of the nodes with a generator.

Our OPF-HGNN has two SageGraph convolution layers followed by relu activations and one final layer with two outputs per generators/external grid nodes (i.e. in the WSCC 9-Bus case 6 outputs). The SageGraph layers are propagated on all the nodes with a mean aggregation; however, the training loss computation only takes into account the generators nodes.

d) *Training and optimization*: We train all the models for 500 epochs and batch size of 128. We use Adam optimizer and a multistep learning rate, starting at 0.1 and decaying by 0.3 at epochs $\in \{250, 375, 450\}$. Data augmentation uses a mutation rate of 0.7 and sets to 1 the weight of the constraint violation penalty λ in equation (6). The predicted active and reactive powers are trained using an MSE loss.

e) *Metrics*: In our empirical study, we report two metrics for the generators and the external grid: Relative Squared Error to the active and reactive powers obtained through the OPF simulation and refer to them as SE_P and SE_Q . We report both the mean and standard deviation of the error on all the validation graphs. In addition, we simulate the power flow using the predicted active and reactive powers and record constraint violations. We report the percentage of predicted graphs that satisfy the constraints in the metric. Better models yield higher CTR and lower $MSE_{P\&Q}$.

B. Comparison with Baselines

We compare in Table II our approach and traditional GNN and FCNN when trained with the same features across three power systems. The main takeaway is that our approach OPF-HGNN achieves high constraint satisfaction across all the power systems, while the alternative approaches's constraint satisfaction collapses with increased size of power grids. For eg., OPF-HGNN achieves 98% constraint satisfaction for 30-bus networks with mutated load powers. In addition to ensuring constraint satisfaction, our approach achieves the lowest MSE in 20/24 scenarios and is up to three order of magnitude more precise than the alternatives. The MSE_P of the active power for graphs with loads mutations is as low as about $1e^{-5}$ for our approach on the 9-bus case.

C. Generalization studies

In this study, we evaluate the generalization capabilities of our approach with few-shot learning and transfer-learning. We summarize our results in Table III.

In the few-shot learning scenarios (scenarios (1), (2), and (3) in Table III), we evaluate the cases where we only have a subset of the training grid (10%) to train on, and evaluate how the performance of the model degrades compared to the full training scenario presented in Table II. For load mutations, the results show no drop in constraint satisfaction between full training and few shot training and a marginal increase in MSE. These results hint that learning the impact of load changes does not require large training sets. There is, however, a significant drop in performances when predicting the OPF with varying generation costs and small training sets. Our results suggest that the impact of power generation costs on OPF optimization is significant and requires ten times more data to effectively learn how to enforce the constraints of the power grid.

Next, we investigate the transfer learning scenarios. We pre-train on the full training set of a source scenario, then fine-tune on 10% of the target scenario. We summarize the results in scenarios (4-7). Our results show that the OPF-HGNN models completely transfer to smaller topologies, with low MSE and high constraint satisfaction. Meanwhile, training on small topologies can fail to generalize to larger topologies, especially with cost mutations. The bottleneck is constraint satisfaction, which seems harder to generalize to larger topologies.

D. Scalability

We compare in Table IV how our models and inference time scale with the size of the system. Our results demonstrate that HGNN complexity is fixed whatever the size of the grid. The inference time scales linearly with the size of the grid. OPF-HGNN requires 4.58ms on one 9-Bus topology and 6.08ms on one 30-Bus topology. HGNN relies on message passing which generalizes with little overhead to large topologies [8].

CONCLUSION AND FUTURE WORK

This paper is the first to formulate the process of learning the AC-OPF as a constrained heterogeneous graph neural network. Our framework, OPF-HGNN, incorporates every component of the power system as a distinct node with its unique feature embedding and boundary constraints.

OPF-HGNN achieves a significant increase in constraint satisfaction of the predicted power systems compared to traditional GNN and FCNN models, especially in larger and more complex grid configurations. Our approach also achieves the lowest MSE in most tested scenarios and is up to 100 times more precise than the GNN approaches for larger grids.

Our extensive empirical study also demonstrates the generalization of our framework with transfer learning and few-shot learning across multiple topologies and mutation distributions.

Our work paves the way for the integration of recent ML breakthroughs, such as self-supervised learning and attention

TABLE II: Comparison of OPF-HGNN, GraphSage GNN, and FCNN. In bold the best values per case.

Approach	Case	Mutation	SE _P MEAN _(STD)		SE _Q MEAN _(STD)		CTR satisfaction
			External Grid	Generators	External Grid	Generators	
OPF-HGNN (our approach)	WSCC 9-Bus	Load	1.77e⁻⁶ _(2.27e⁻⁶)	2.97e⁻⁶ _(4.10e⁻⁶)	2.49e⁻¹ _(3.12e⁻¹)	2.60e⁻⁵ _(1.68e⁻⁴)	1.00
		Cost	2.58e⁻⁵ _(4.21e⁻⁵)	1.28e⁻⁵ _(2.31e⁻⁵)	4.74e⁻⁵ _(2.23e⁻⁴)	4.66e⁻⁵ _(3.55e⁻⁴)	0.94
	IEEE 14-Bus	Load	1.72e⁻⁵ _(2.76e⁻⁵)	4.63e ⁻² _(6.91e⁻¹)	7.62e ⁻² _(1.53e⁻³)	8.65e ⁻³ _(2.00e⁻³)	0.83
		Cost	2.02e⁻³ _(3.31e⁻³)	9.81e ⁻³ _(1.49e⁻²)	1.83e⁻² _(3.95e⁻²)	1.43e⁻⁵ _(1.66e⁻⁴)	1.00
	IEEE 30-Bus	Load	4.23e⁻⁵ _(1.08e⁻⁴)	9.24e⁻⁶ _(1.94e⁻⁵)	8.92e⁻⁵ _(4.22e⁻⁵)	1.28e⁻⁵ _(1.16e⁻³)	0.98
		Cost	5.89e⁻³ _(5.37e⁻²)	2.97e⁻³ _(1.03e⁻²)	6.62e⁻⁵ _(1.23e⁻⁴)	4.59e⁻⁵ _(4.57e⁻⁴)	0.95
GraphSage GNN	WSCC 9-Bus	Load	1.02e ⁻⁴ _(1.27e⁻⁴)	3.74e ⁻⁵ _(5.44e⁻⁵)	2.49e ⁻¹ _(3.12e⁻¹)	3.83e ⁻² _(1.17e⁻¹)	1.00
		Cost	1.32e ⁻³ _(2.35e⁻³)	3.85e ⁻³ _(1.08e⁻²)	9.23e ⁻² _(3.56e⁻¹)	3.42e ⁻² _(1.38)	0.75
	IEEE 14-Bus	Load	2.29e ⁻³ _(3.99e⁻³)	4.71e ⁻² _(2.77e⁻¹)	9.30e ⁻³ _(4.72e⁻³)	4.44e⁻³ _(6.18e⁻³)	0.87
		Cost	1.37e ⁻² _(2.33e⁻¹)	1.49e ⁻³ _(8.63e⁻²)	2.09e ⁻² _(1.26e⁻¹)	1.44e ⁻² _(4.62e⁻¹)	0.06
	IEEE 30-Bus	Load	7.07e ⁻⁴ _(2.68e⁻³)	1.98e ⁻³ _(7.71e⁻³)	4.20e ⁻² _(8.86e⁻²)	5.98e ⁻³ _(5.83e⁻¹)	0.39
		Cost	2.26e ⁻² _(1.31e⁻¹)	1.21e ⁻² _(1.08)	2.28e ⁻² _(1.49e⁻¹)	4.41e ⁻² _(1.32)	0.01
FCNN	WSCC 9-Bus	Load	1.51e ⁻⁵ _(1.32e⁻⁴)	1.58e ⁻⁵ _(2.01e⁻⁵)	1.05e ⁻¹ _(1.39e⁻¹)	1.57e ⁻² _(5.20e⁻²)	1.00
		Cost	2.86e ⁻⁴ _(9.18e⁻⁴)	1.37e ⁻³ _(4.26e⁻³)	1.55e ⁻³ _(1.44e⁻²)	3.38e ⁻² _(4.19e⁻¹)	0.64
	IEEE 14-Bus	Load	2.45e ⁻⁴ _(1.19e⁻³)	4.46e⁻² _(1.51e⁻¹)	1.41e⁻³ _(4.38e⁻²)	6.45e ⁻³ _(9.56e⁻³)	0.02
		Cost	2.89e ⁻² _(1.25e⁻¹)	6.95e⁻³ _(9.42e⁻²)	8.43e ⁻² _(5.60e⁻¹)	7.68e ⁻³ _(6.89e⁻²)	0.18
	IEEE 30-Bus	Load	1.93e ⁻² _(2.71e⁻¹)	4.55e ⁻³ _(1.33e⁻²)	7.40e ⁻³ _(2.78e⁻²)	2.27e ⁻² _(2.16e⁻¹)	0.42
		Cost	2.09e ⁻¹ _(1.35)	3.06e ⁻¹ _(4.08)	4.48e ⁻² _(2.42e⁻¹)	2.94e ⁻¹ _(40.48)	0.00

TABLE III: Mean and Standard deviation of relative SE in few-shot and transfer learning scenarios.

ID	Cases	Mutation	SE _P MEAN _(STD)		SE _Q MEAN _(STD)		CTR satisfaction
			External Grid	Generators	External Grid	Generators	
(1)	9-Bus → 9-Bus	Load	2.15e ⁻⁶ _(3.40e⁻⁶)	9.77e ⁻⁴ _(1.51e⁻³)	7.85e ⁻⁶ _(1.24e⁻⁵)	5.08e ⁻² _(1.68e⁻¹)	1.00
		Cost	4.33e ⁻³ _(1.91e⁻²)	3.81e ⁻³ _(9.05e⁻³)	2.87e ⁻³ _(8.96e⁻³)	1.48e ⁻¹ _(1.86)	0.76
(2)	14-Bus → 14-Bus	Load	4.98e ⁻⁴ _(5.78e⁻⁴)	2.48e ⁻² _(2.52e⁻¹)	3.57e ⁻² _(2.44e⁻²)	1.07e ⁻² _(1.88e⁻²)	0.84
		Cost	1.30e ⁻² _(3.59e⁻²)	5.10e ⁻² _(1.01e⁻¹)	4.58e ⁻² _(8.73e⁻²)	1.13e ⁻³ _(1.16e⁻²)	0.52
(3)	30-Bus → 30-Bus	Load	6.46e ⁻⁵ _(2.54e⁻⁴)	7.86e ⁻⁴ _(1.86e⁻³)	2.13e ⁻¹ _(4.35e⁻⁴)	6.47e ⁻⁴ _(5.23e⁻³)	0.96
		Cost	1.53e ⁻² _(2.90e⁻²)	1.31e ⁻² _(4.14e⁻²)	7.74e ⁻⁴ _(6.32e⁻³)	4.59e ⁻⁴ _(8.25e⁻³)	0.73
(4)	9-Bus → 14-Bus	Load	7.44e ⁻⁶ _(1.12e⁻⁵)	3.50e ⁻¹ _(1.60)	7.46e ⁻³ _(4.18e⁻³)	2.50e ⁻² _(3.73e⁻²)	0.00
		Cost	1.80e ⁻² _(6.20e⁻²)	4.95e ⁻² _(5.87e⁻¹)	4.36e ⁻² _(1.11e⁻¹)	7.08e ⁻¹ _(6.78)	0.17
(5)	9-Bus → 30-Bus	Load	1.42e ⁻⁴ _(2.98e⁻³)	1.35e ⁻² _(3.44e⁻²)	3.39e ⁻⁵ _(2.78e⁻⁴)	4.39e ⁻³ _(1.74e⁻²)	0.98
		Cost	3.96e ⁻² _(1.67e⁻¹)	4.04e ⁻² _(1.16e⁻¹)	2.72e ⁻³ _(7.32e⁻³)	1.02e ⁻³ _(9.00e⁻²)	0.35
(6)	14-Bus → 9-Bus	Load	1.61e ⁻¹ _(2.01e⁻¹)	3.87e ⁻³ _(4.76e⁻³)	2.86e ⁻² _(8.10e⁻²)	8.76e ⁻² _(3.20e⁻¹)	1.00
		Cost	1.42e ⁻³ _(3.41e⁻³)	3.61e ⁻² _(8.43e⁻²)	6.44e ⁻⁴ _(1.04e⁻²)	2.71e ⁻² _(1.50)	0.75
(7)	30-Bus → 9-Bus	Load	3.16e ⁻⁵ _(1.57e⁻⁴)	1.22e ⁻⁴ _(1.75e⁻⁴)	6.09e ⁻³ _(1.11e⁻²)	3.36e ⁻⁴ _(7.07e⁻²)	1.00
		Cost	2.82e ⁻⁴ _(6.90e⁻⁴)	7.47e ⁻³ _(2.37e⁻²)	1.88e ⁻³ _(9.74e⁻³)	7.55e ⁻³ _(3.35e⁻²)	0.84

TABLE IV: Graph NN model size (trainable weights) and inference time for 100.000 grids on CPU

Size	Case9		Case14		Case30	
	Size	Time (sec)	Size	Time (sec)	Size	Time (sec)
555,052	458.46	555,052	560.88	555,052	607.61	

mechanisms, specifically tailored to address complex challenges in the power grid. The generalizable framework presented in this paper represents a blend of theoretical innovation and practical application to transform power grid operations, enhancing accuracy, reliability, and efficiency.

REFERENCES

- [1] B. Donon, R. Clément, B. Donnot, A. Marot, I. Guyon, and M. Schoenauer. Neural networks for power flow: Graph neural solver. *Electric Power Systems Research*, 189:106547, Dec. 2020.
- [2] W. L. Hamilton, R. Ying, and J. Leskovec. Inductive representation learning on large graphs, 2018.
- [3] F. Hasan, A. Kargarian, and A. Mohammadi. A Survey on Applications of Machine Learning for Optimal Power Flow. In *2020 IEEE Texas Power and Energy Conference*, pages 1–6, Feb. 2020.
- [4] B. Huang and J. Wang. Applications of Physics-Informed Neural Networks in Power Systems - A Review. *IEEE Transactions on Power Systems*, 38(1):572–588, Jan. 2023.
- [5] B. K. Karmakar and A. K. Pradhan. Detection and classification of faults in solar pv array using thevenin equivalent resistance. *IEEE Journal of Photovoltaics*, 10(2):644–654, 2020.
- [6] H. Khorasgani, A. Hasanzadeh, A. Farahat, and C. Gupta. Fault detection and isolation in industrial networks using graph convolutional neural networks. pages 1–7, 06 2019.
- [7] T. N. Kipf and M. Welling. Semi-supervised classification with graph convolutional networks, 2017.
- [8] W. Liao, B. Bak-Jensen, J. Radhakrishna Pillai, Y. Wang, and Y. Wang. A Review of Graph Neural Networks and Their Applications in Power Systems. *Journal of Modern Power Systems and Clean Energy*, 2022.
- [9] S. Liu, C. Wu, and H. Zhu. Topology-Aware Graph Neural Networks for Learning Feasible and Adaptive AC-OPF Solutions. *IEEE Transactions on Power Systems*, 38(6):5660–5670, Nov. 2023.
- [10] D. Owerko, F. Gama, and A. Ribeiro. Optimal Power Flow Using Graph Neural Networks. In *2020 IEEE International Conference on Acoustics, Speech and Signal Processing*, Barcelona, Spain, May 2020. IEEE.
- [11] T. Simonetto, S. Dyrnishi, S. Ghamizi, M. Cordy, and Y. L. Traon. A unified framework for adversarial attack and defense in constrained feature space, 2022.
- [12] T. Simonetto, S. Ghamizi, A. Desjardins, M. Cordy, and Y. L. Traon. Constrained adaptive attacks: Realistic evaluation of adversarial examples and robust training of deep neural networks for tabular data, 2023.
- [13] L. Thurner, A. Scheidler, F. Schafer, J. H. Menke, J. Dollichon, F. Meier, S. Meinecke, and M. Braun. pandapower - an open source python tool for convenient modeling, analysis and optimization of electric power systems. *IEEE Transactions on Power Systems*, 2018.